AN ABSTRACT OF THE THESIS OF

Stephen L. Albright for the degree of Master of Science in Mechanical Engineering presented on December 6, 1984.

Title: An Experimental Investigation into the Dynamic Collapse Phase of Drilling Fluid Discharged into a Stratified, Flowing Environment

Redacted for Privacy

Abstract approved:_____

Dumping drilling mud from offshore drilling rigs into the ocean could have a negative impact on the marine environment. Due to this possible impact, the Offshore Operators Committee (OOC) has deemed it necessary to predict the fate of drilling mud discharged into the ocean. Through the funding of OOC and Exxon Production Research Company, a computer program was developed which models the fate of discharged drilling mud for a wide variety of ocean conditions. At present, the program has been through a limited amount of testing and still contains modeling coefficients whose validity have not been established.

A laboratory simulation of mud discharging into a flowing, stratified environment was designed and tested in the Mechanical Engineering facilities at Oregon State University. The objective of this experiment was to observe and quantitatively describe the behavior of the dynamic collapse phase of the mud. The primary emphasis was given to the shape and position of mud-plume cross

sections as they progressed into the dynamic collapse phase. Using a collimated light source and motor driven camera, each cross section was captured on film. Photographs showed that the behavior of the discharged-mud simulation closely matched actual mud discharges into the ocean. It is considered that the measured results would serve as a good check against the OOC computer program's ability to model the dynamic collapse phase of discharged mud.

An Experimental Investigation into the Dynamic Collapse Phase of Drilling Fluid Discharged into a Stratified, Flowing Environment

by

Stephen L. Albright

A THESIS

submitted to

Oregon State University

in partial fulfillment of
the requirements for the
degree of

Master of Science

Completed December 6, 1984

Commencement June 1985

APPROVED:

Redacted for Privacy

Major Professor, Dr. Lorin Davis, Mechanical Engineering

Redacted for Privacy

Mechanical Engineering, Department Head, Dr. James Welty

Redacted for Privacy

Dean of Graduate School

Date thesis is presented December 6, 1984

TABLE OF CONTENTS

LIST OF FIGURES

LIST OF TABLES

LIST OF SYMBOLS

Symbol	Expression	Symbol Description
A		cross sectional area of plume
b		semi-major axis of plume
D		discharge pipe diameter
Fr	$Uo/[gD\Delta\rho_o/\rho_c]^{1/2}$	Densimetric Froude Number: ratio of inertial to bouyant forces
g		acceleration of gravity
R	Ua/Uo	Velocity Ratio
Uo		discharge velocity
Ua		towing (current) velocity
X		horizontal distance from source parallel to direction of tow
Y		vertical distance from source
Z		horizontal distance from source perpendicular to direction of tow
ρ_a		ambient density
ρ_o		mud density
$\Delta\rho_o$	$\rho_o-\rho_a$	difference between mud density and ambient density

An Experimental Investigation into the Dynamic Collapse Phase of Drilling Fluid Discharged into a Stratified, Flowing Environment

INTRODUCTION

The offshore drilling industry in recent years has been faced with developing concerns over the impact it may have on the marine environment. A particular area of concern is the fate and effect of discharged drilling fluids (mud).

Drilling mud has various applications. It is used as a bit lubricant, as a coolant, for pressure control and as a transport medium to bring cuttings to the surface. The mud is periodically discharged into the ocean during drilling operations and is dumped in bulk after exploratory drilling. Once in the ocean, the mud disperses in various ways depending on ocean conditions such as currents, density gradient and dynamic characteristics of the mud's own inertia. To assess the impact, several studies have been conducted concerning the environmental fate and effect of drilling mud. In determining the fate of drilling mud, attention has been given to the physical discharge phenomenon and the concentration of drilling mud components that can be found in the discharge region. Individual site studies have offered much insight into the behavior and fate of mud discharges.

In a study done in Tanner Bay, off the coast of Los Angeles, California, Ray and Meek [1] found mud discharges were diluted from 500-5800:1 within three meters of discharge. They also found,

through divers' observations, the discharged materials separated in three directions: upward, downward and horizontally. Heavier material began an immediate vertical drop. Aggregates of some flocculated (i.e. particles clinging together in a clump) mud also fell straight downward. The lighter particles rose slightly upward and drifted horizontally with the current.

In the Gulf of Mexico, Ayers and Sauer [2] observed the discharged mud formed two plumes as it entered the water column, an upper plume and a lower plume. The lower plume descended rapidly and had a small, roughly cylindrical diameter. As it descended, the plumeentrained surrounding fluid and grew until it hit the bottom. Upon impact, the lower plume formed a fluffy cloud that spread slowly along the bottom. Another behavior of the plume is explained by Koh [3] in a summary of the physics related to mud. He states that because of the continuous mixing which occurs, a sinking plume may terminate its decent before the diluted waste reaches the bottom if there is sufficient density stratification in the receiving water. This is called stratification trapping.

Although field studies and observations have been useful in helping to understand the fate of drilling discharges, the results may not always be applicable to other sites or other sets of discharge conditions. Hence arose the need for a general computer model to permit operators and regulatory agencies to predict the fate of drilling discharges at other sites under a variety of discharge conditions.

Brandsma, Davis, Ayers and Sauer [4] developed such a program

from earlier models for dredged material discharges. It had the ability to reproduce several observed features of drilling mud discharges but did not consistently produce closely correlated mud-concentration data with field-test data of the same type. However, further work was encouraged since the program was still in a developmental phase.

The Offshore Operators Committee (OOC) and Exxon Production Research Company continued to support the program to its present stage of development. This program, developed by Brandsma, Ayers and Sauer [5], places emphasis on predicting the fate of a wide range of particle-sized mud solids discharged at various rates of several minutes duration into an environment having variable currents, variable depths, and variable density stratification. Among other features, the program models three distinct discharge phases: convective descent (jet phase), dynamic collapse and passive diffusion. The jet phase begins as the mud is first discharged into the ambient. The mud entrains the surrounding fluid as it descends and bends in the direction of the ambient current.

The jet phase ends and dynamic collapse begins when the plume reaches a level of neutral bouyancy or hits the bottom, at which point the descent stops and horizontal spreading is predominant. When dynamic collapse occurs due to ambient density stratification (i.e. reaches equilibrium at a level of neutral bouyancy), the material in the lower region of the plume is lighter than the surrounding fluid and tends to rise. Similarly, the material in the upper region is heavier than the surrounding fluid and tends to

fall. This forces the plume to move laterally and spread. It is somewhat like taking a flexible circular ring and pinching it at opposite sides with your thumb and forefinger. These dynamic forces causing the collapse tend to die out and the spreading due to turbulent diffusion becomes dominate. At this point the collapse phase ends and the passive diffussion phase begins. The three phases are pictured in figure 1.

Through the first two phases, various classes of solid particles settle out of the main plume. The settling velocities of the solids are dependent upon the ionic strength of the medium in which they settle. Smaller solid particles have a tendency to flocculate in salt water. The settling velocity of these flocculated units differs from the settling velocity of the individual particles that make them up.

The OOC computer program's ability to accurately model the above described plume behavior is dependent on the use of many empirically derived coefficients, some of which are better established than others. For one to have confidence in these coefficients they must be checked. A method of obtaining this information without the problems associated with field tests is laboratory simulation. One such experiment was conducted by Mohebbi and Davis [6]. The primary concern of their laboratory simulation was the dilution characteristics of the plume in the water column and the material settled on the bottom. A Comparison of the total solid concentration calculated by the OOC computer model with experimental results showed good agreement.

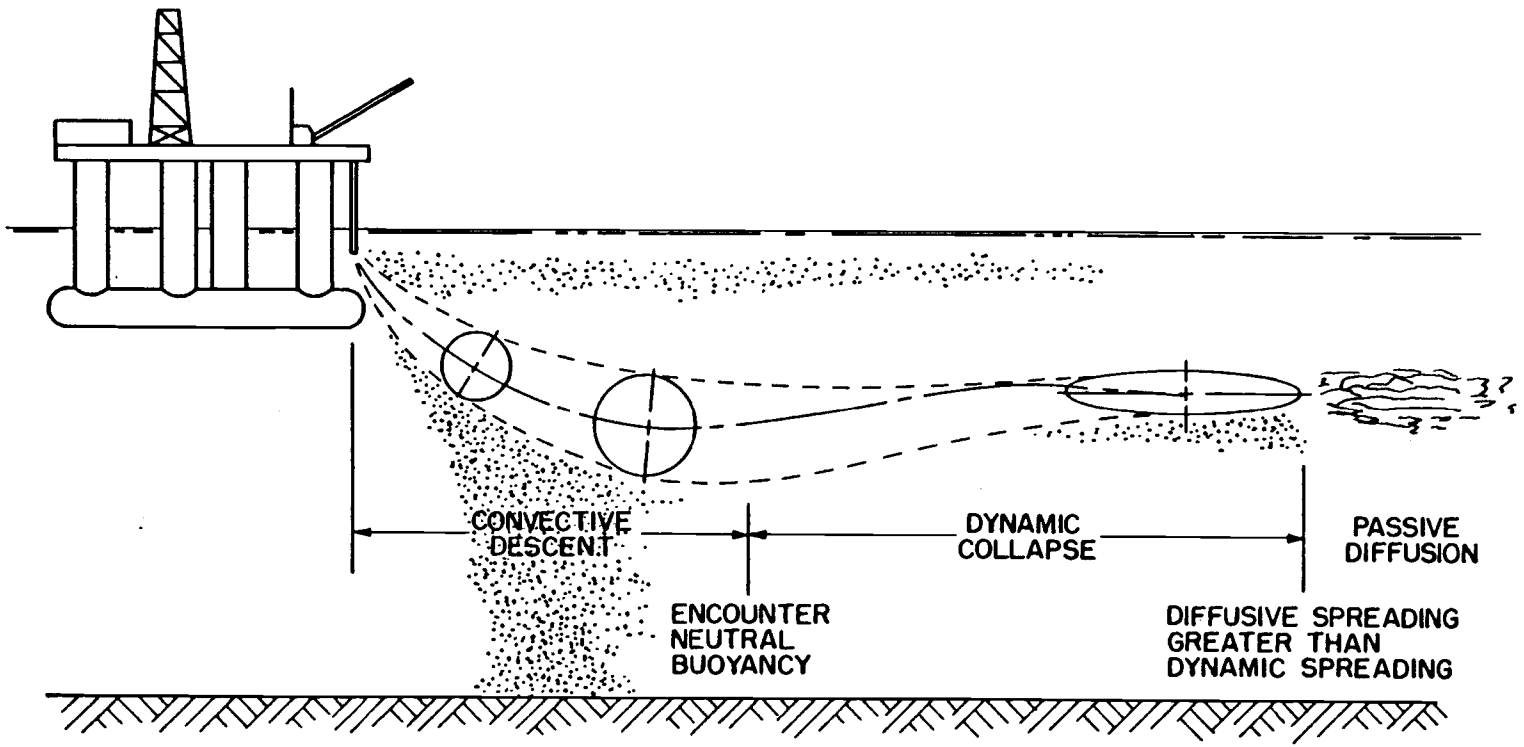

Figure 1. Three phases of discharged mud plume.

In the jet phase of the OOC model, the entrainment coefficients are well established by experimental investigation. In the dynamic collapse phase, however, the coefficients used to model the forces opposing the inertial forces of the spreading plume are not well established. These are the drag and friction coefficients. The drag and friction coefficients currently used in the OOC program were obtained from the plume modeling work of Koh and Chang [7]. The drag coefficients are based on flow over a spheroidal wedge in the Z direction and flow normal to a circular plate in the Y direction (see plume coordinates, figure 11.). The friction coefficient is based on an "educated guess." The values used are subject to revision since they are not strictly applicable to a discharged mud plume. These difficiencies show the need for further experimental study into the dynamic phases of discharged mud as a check against the OOC computer model's coefficients.

The objective of this experimental investigation was to develop a method to observe and quantitatively describe the behavior of the dynamic collapse phase of drilling mud discharged vertically downward into a stratified, flowing ambient. The primary emphasis was given to the shape and position of various plume cross sections as they progressed into the dynamic collapse phase.

The basic laboratory simulation involved the discharge of mud down through a tube into a large tank (towing channel) filled with salt water in the lower region and fresh water in the upper region of the channel. This step density gradient was used to produce a collapse of the mud plume before it reached the bottom of the

channel. As the mud was discharged, the tube moved horizontally at a constant velocity down the center of the channel to simmulate a current. With a collimated light, mirrors and a camera, cross sections of the developing plume were captured on film and their shape and position measured. The experiment was conducted for three salinities of the lower salt water layer (32, 19, and 12.5 parts per thousand) to observe the effect of different gradients. The measured results could later be compared with results of a computer simulation which uses similar discharge conditions as input.

EXPERIMENTAL TECHNIQUE

In this chapter the experimental equipment, procedure and measuring technique is described.

Equipment

The drilling mud used in the experiments was provided by Exxon Production Research Company and was the same mud used by Mohebbi in his experiments [6]. It had a specific gravity of 1.184 and a composition of 12 percent by weight high-gravity solids (BaSO4), 15.2 percent low-gravity solids (clays) and 72.8 percent water.

The towing channel measured 12.2 m long, 0.61 m high, and 0.91 m wide. Its walls were made of 1.25 cm thick plexiglass braced by square steel tubing. Its floor consisted of a 2.54 cm steel plate. A carriage containing the discharge apparatus was towed along rails above the channel by a cable and variable speed motor.

The discharge apparatus included an acrylic tank (55 x 50 x 17.5 cm) to carry the mud, a mud pump and variable speed motor, and a 1.57 cm I.D. discharge tube attached to a small box-shaped plenum. The tube extended 2 cm below the surface and was positioned at center width of the towing channel. The plenum attached to the discharge tube dampened the pulsating movement of the mud coming from the pump. The complete arrangement of this apparatus is shown on figure 2.

To get the desired salt water gradient in the towing channel a 275 gallon plastic tank was used to premix salt and water. The salt

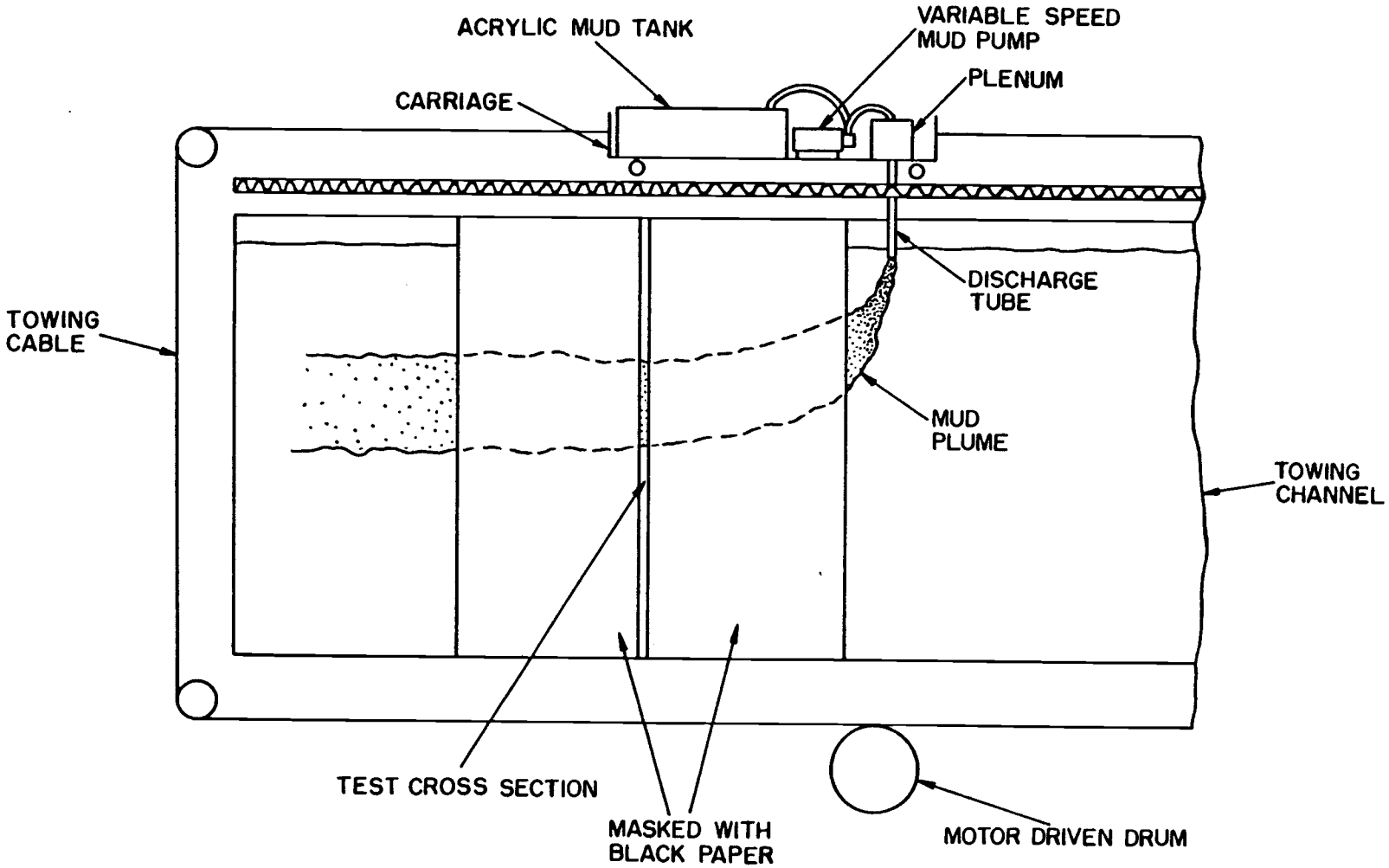

Figure 2. Towing channel and motor driven carriage with discharge apparatus.

water mixture was pumped from the bottom of the mixing tank through 3.81 cm PVC pipe to the bottom of the towing channel. A valve down stream of the pump was used to regulate the flow of salt water. By slowly pumping salt water into the towing channel previously filled half way with fresh water, a step gradient could be created with very little mixing of the two fluids.

The salinity of the salt water mixture was measured using a conductivity probe connected to a carrier amplifier and oscilloscope. The carrier amplifier is typically used for strain gage calibration. However, in this case it was used to measure conductance. The best resolution was obtained when setting the amplifier to 5kμstrain/division. Each division on the oscilloscope at this setting was related to a particular salinity. The conductivity probe was then calibrated from six salt water samples of known salinity. The salinity of these samples was measured using a salinometer operated by the School of Oceanography at Oregon State University. The salinometer is accurate to the nearest part per million. Whereas the best accuracy obtained from the conductivity probe was 0.5 parts per thousand (ppt). Using the samples and conductivity probe, a calibration curve was drawn for salinity vs. oscilloscope divisions. One such curve is shown in figure 3.

A photographic technique was used to measure a progression of cross sections of the mud plume . The technique was much the same as used by Davis, Gregoric and Bushnell [8]. This experiment involved photographing merging isothermal jets in a cross flow

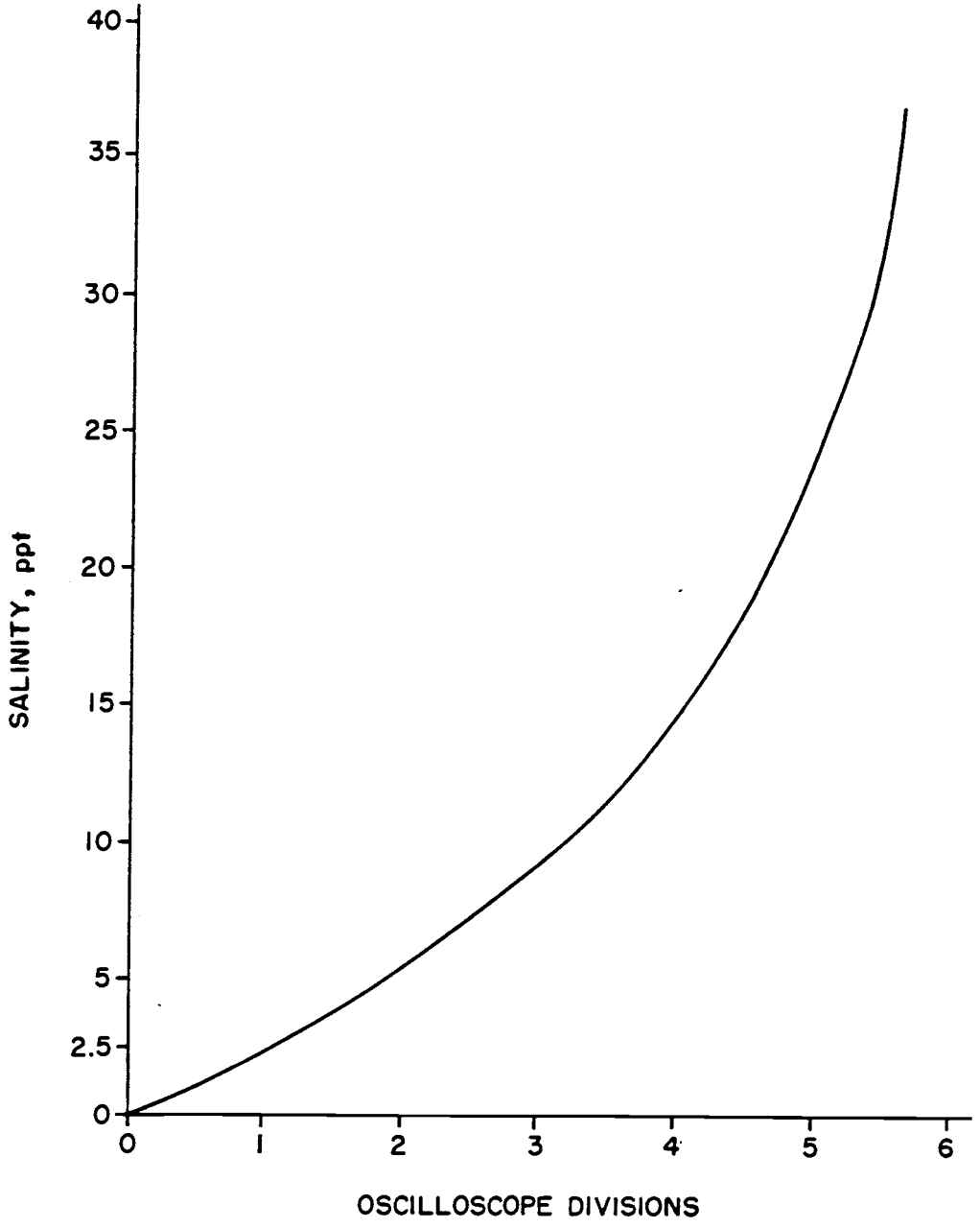

Figure 3. Calibration curve of salinity vs. oscilloscope divisions for run # 6.

environment. They used a vertically collimated light which passed through the towing channel widthwise and illuminated a cross section of the plume. Since both the jet and ambient fluids were clear, a dye was used in the discharged fluid to reflect the light. A mirror was placed a short distance down stream from the light at a 45 degree angle between the channel walls. A camera mounted on a tripod outside the channel was focused on the reflected image of the illuminated plume cross section.

This photographic scheme had a problem when discharging mud instead of a clear fluid. The discharged mud coming toward the mirror blocked most of the illumated cross section. To circumvent this, two mirrors were used so the plume could be viewed from the side at an acute angle. The first mirror was placed against the channel wall 90 degrees and adjacent to the light column. A second mirror was placed 60 degrees from the channel wall and 0.85 m from the light column. This afforded a view of the plume 30 degrees from a front view, making the outer edge of the mud plume cross section visible.

The collimated light was created using 4-500 W stage lamps, two placed on either side of the channel. The mirror and lamp arrangement is shown in figure 4. The outer channel walls in the regions of the lights were masked off in black with the exception of a 3 mm wide vertical slit. A thin piece of sheet metal with a vertical slot in the center was placed in front of the lens of each stage light to eliminate unwanted light.

The photographing was done at night to enhance the contrast

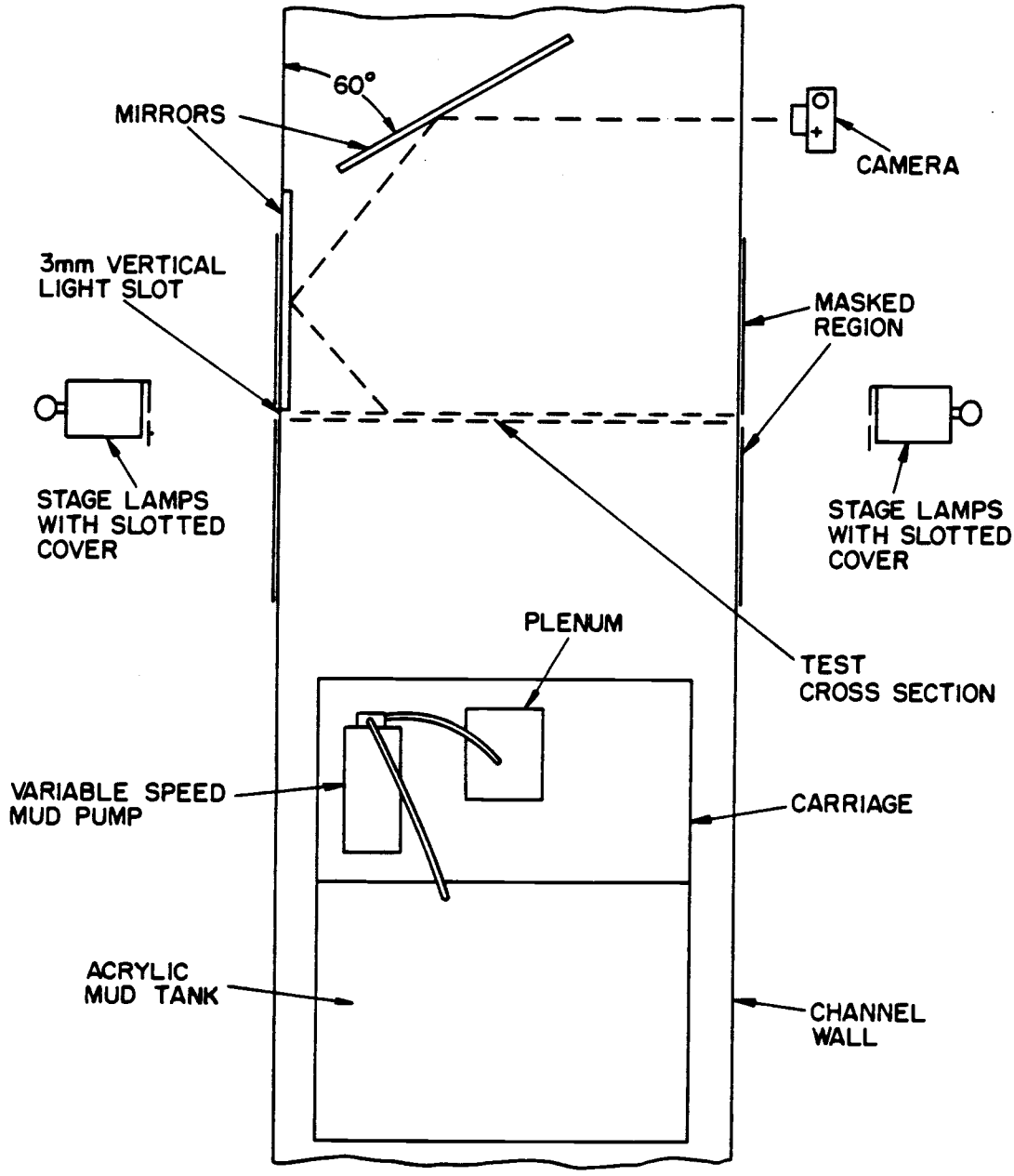

Figure 4. Photographic set up from a top view of the towing channel.

of the illuminated image. Black and white 400 ASA film with an exposure latitude of 50-1600 ASA was used. The film was exposed at f1.4 and a shutter speed of 1/30 sec.. At slower shutter speeds the image definition was poor.

Procedure

Usable data were obtained from four runs. In each run, the mud discharge rate and towing rate were preset to desired levels. The salinity of the salt water in the lower half of the channel differed in three of the four runs. The salinities were: 32 ppt for run 6, 19 ppt for run 7 and 12.5 ppt for runs 8 and 9. There was a little mixing of salt water with fresh water after filling. This resulted in a small transition band going from fresh water to full salinity. The salinity gradient for each of the four runs is shown graphically in figure 5.

The experimental procedure for each run was as follows:

1) The mirrors were set in the channel at their proper positions.
2) The stage lamps were turned on to check for the right alignment then shut off.
3) The towing channel was filled half way with fresh water.
4) Salt and water were mixed in the mixing tank to the desired salinity.
5) The salt water was pumped to the bottom of the towing channel at an average rate of 1.8 gpm. The slow rate minimized mixing of the two fluids.

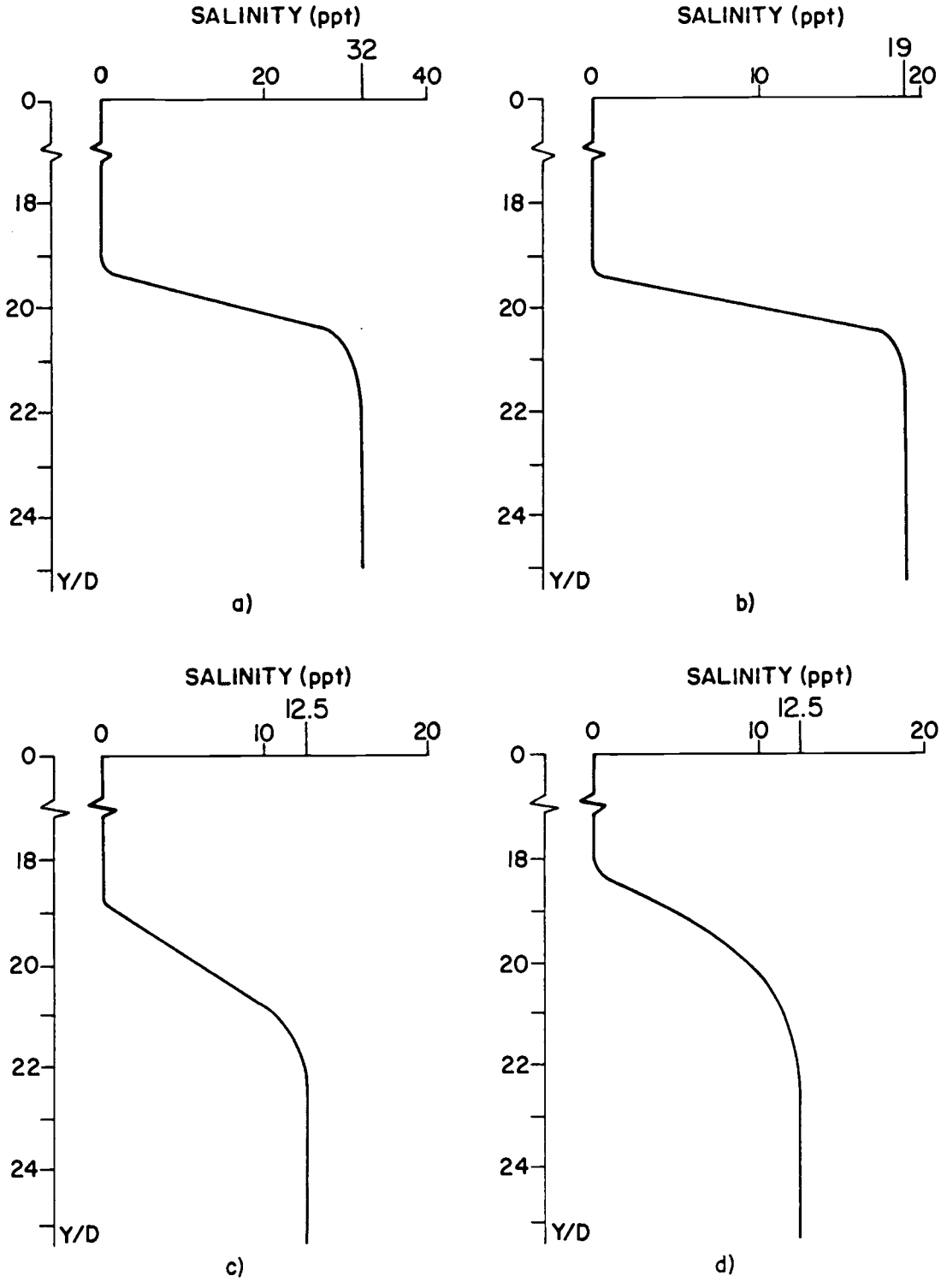

Figure 5. Salinity profiles; a) run # 6, b) run # 7
c) run # 8, d) run # 9

6) The salinity samples were floated in the towing channel for approximately an hour and a half to equalize their temperatures with the fluid in the channel. The bath was approximately 21 degrees centigrade. The conductivity probe was calibrated using the samples, after which the salinity of the fluid in the channel was measured at various depths, Y. The probe was then recalibrated to check for any change.

7) To measure the plume cross section a T-shaped rod with markings at 2 cm intervals was placed in the center of the channel in the path of the light column. The camera was focused on the measuring rod and a picture was taken. The rod was then removed.

8) The drilling mud was thoroughly mixed using a propeller blade and an electric drill. After all mud particles were suspended and the consistency uniform, the mud was poured into the towing carriage tank.

9) The carriage speed was adjusted to the desired level, the mud pump set to full speed, and the camera set to f1.4, 1/30 sec..

10) The stage lamps were turned on and the laboratory lights turned off. The mud pump and towing motor were both started. Tape markings on the carriage and rails of the towing channel indicated the position of the discharge tube relative to the collimated light. At the first mark a stop watch was started. The discharge tube and the

light column were at the same position at the second mark. Using an auto-winder the camera's shutter was released at the second mark and twelve additional marks at 5 cm intervals. At the last mark, 250 cm from the first, the watch was stopped.

11) All lights were turned on and the channel was drained and cleaned.

12) The film was removed from the camera and turned in for development.

The developed photos from runs 6 to 9 are shown in figures 6 to 9 respectively. In observing the photos one can see the plume collapsing and spreading. The low-gravity particles stay a drift while the high-gravity particles fall from the collapsed region and then flocculate as they continue to the bottom.

Measurement

Five dimensionless variables were used to describe the relative position and geometry of the plume cross section. These were: X/D, the horizontal distance from the discharge tube to the plume cross section; Y/D, the vertical distance from the discharge tube to the center line of the plume cross section; Ymax/D, the vertical distance from the discharge tube to the lower most edge of the plume cross section excluding the flocculated units settling out; b/D, the horizontal distance perpendicular to tow direction from the discharge tube to the outer most edge of the plume cross section; and $A/(\pi D^2/4)$, the area of the plume cross section. The dimensionless plume coordinates are shown in figure 10.

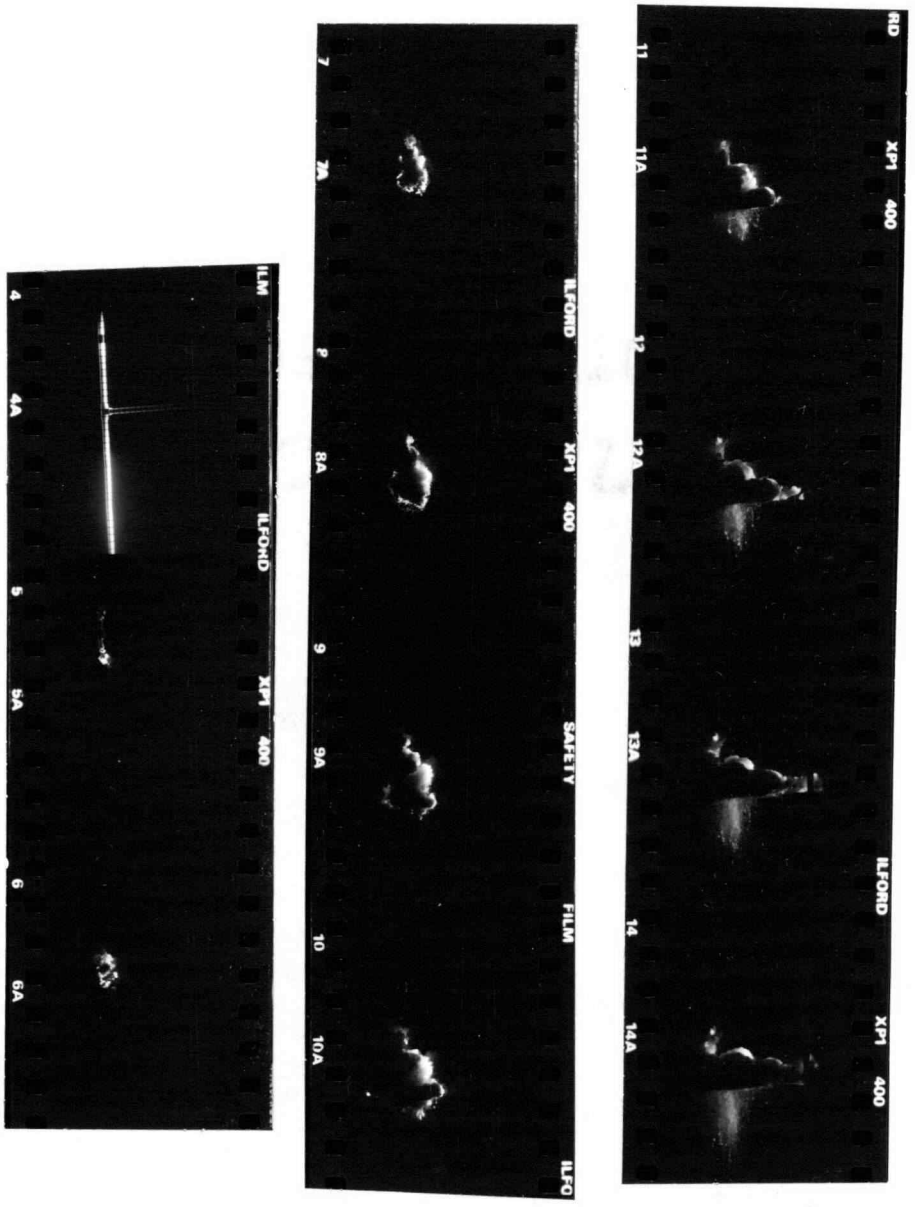

Figure 6. Contact print for run #6.

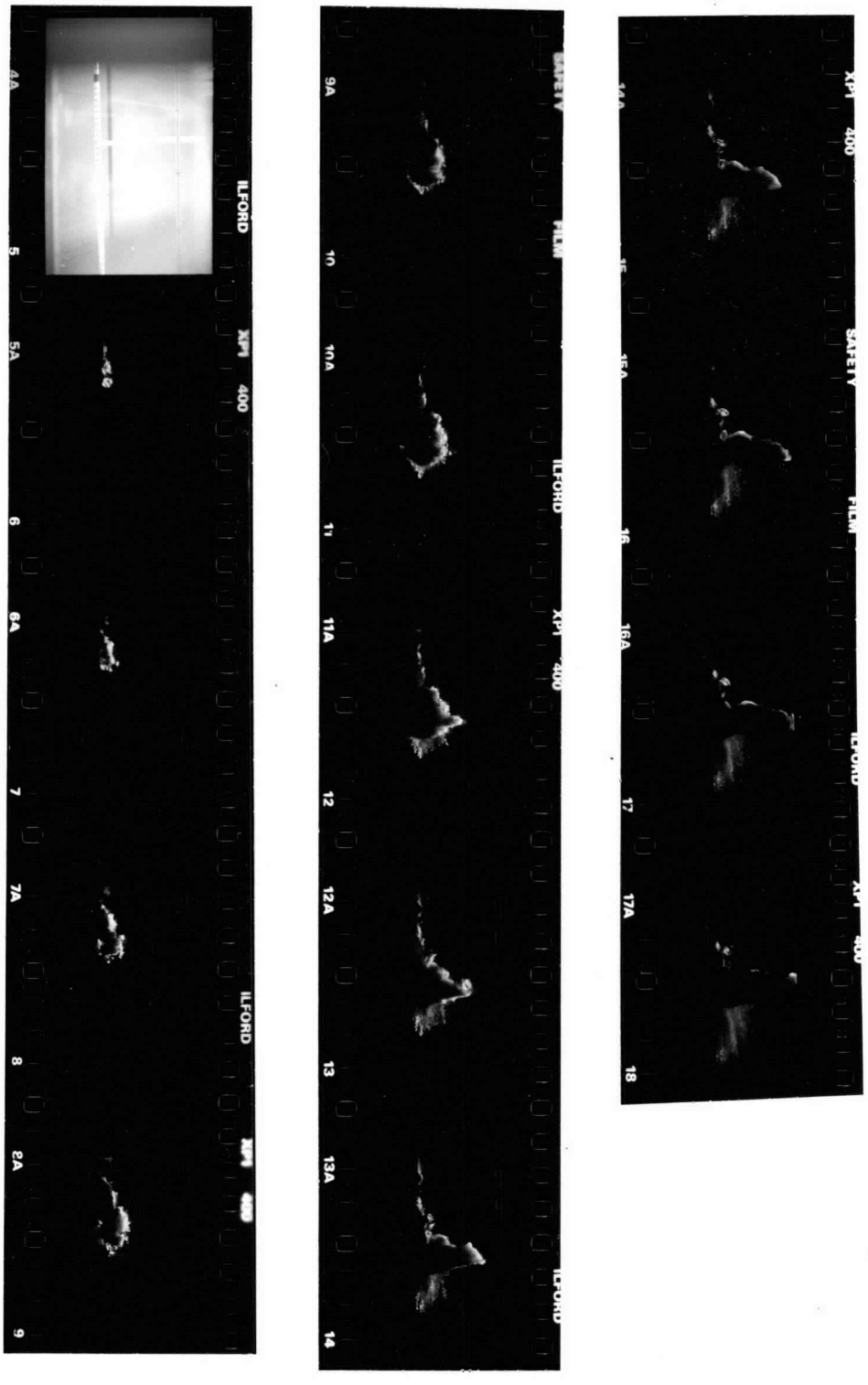

Figure 7. Contact print for run #7.

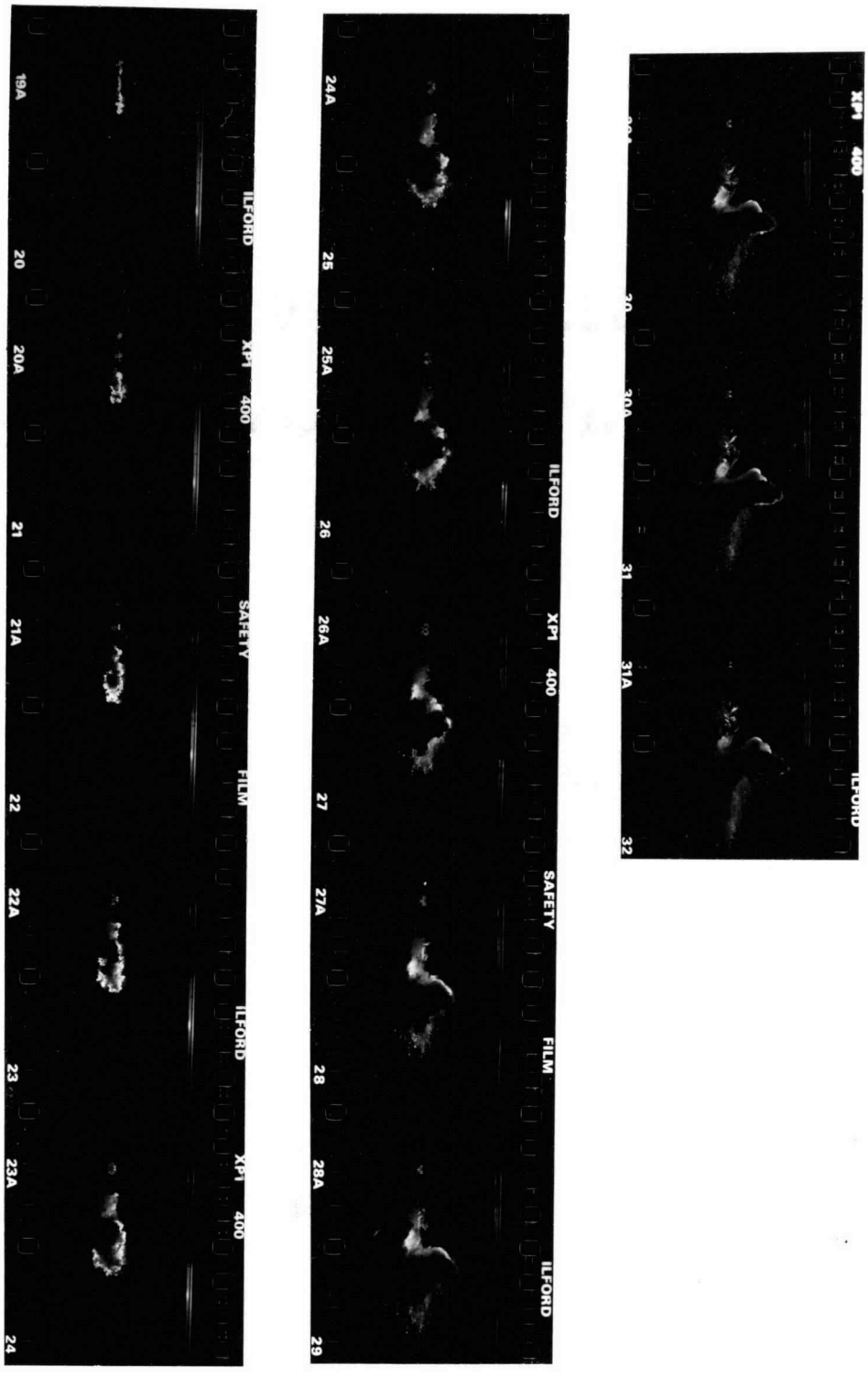

Figure 8. Contact print for run #8.

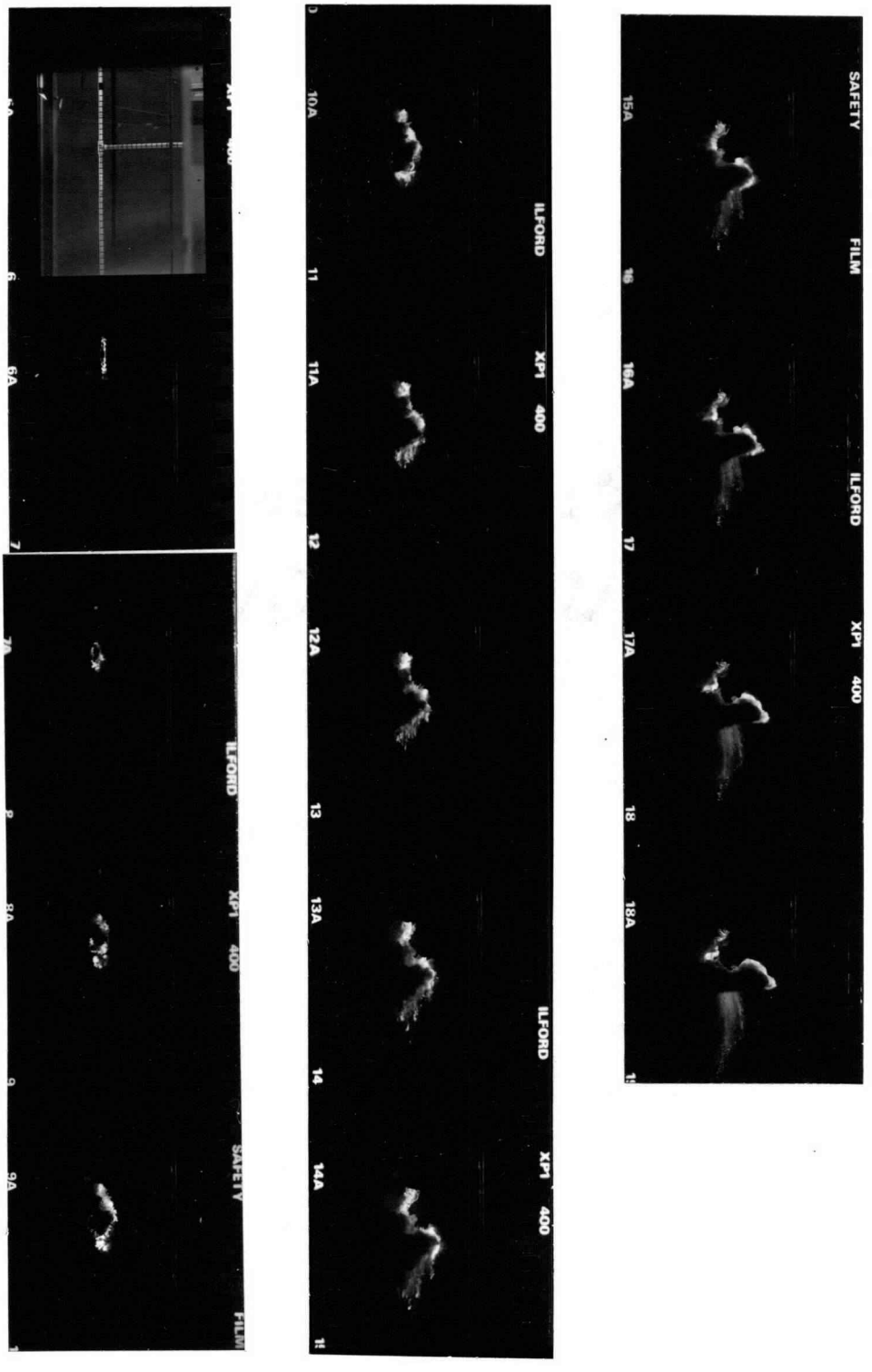

Figure 9. Contact print for run #9.

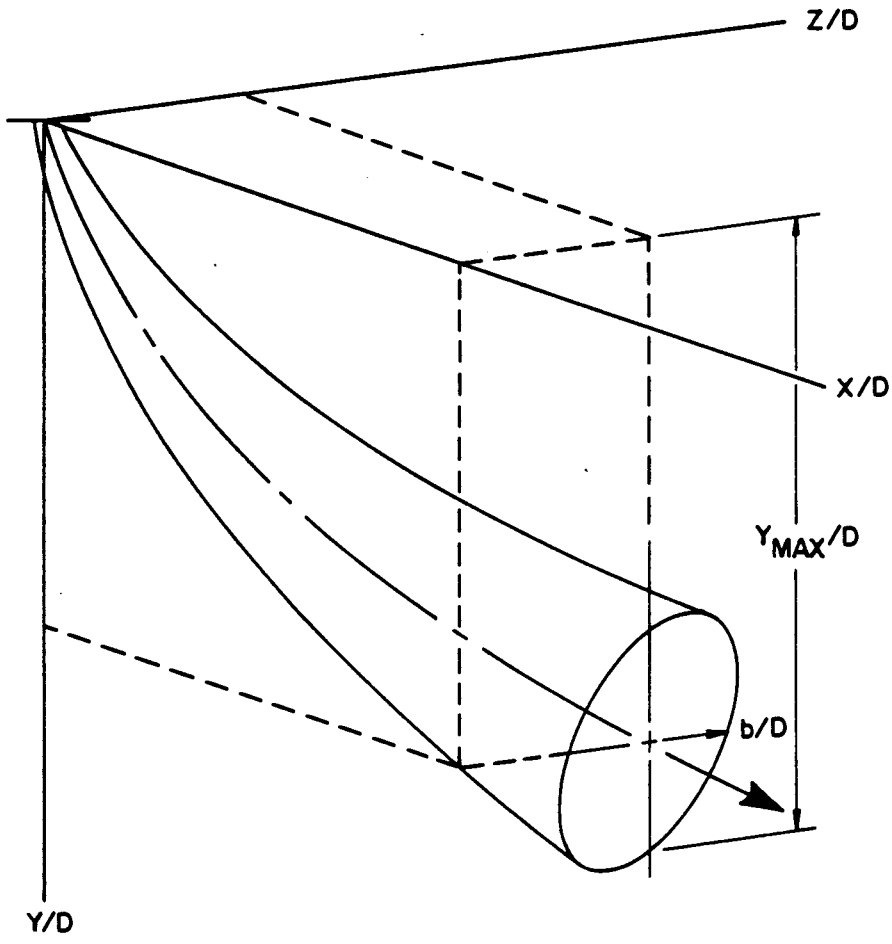

Figure 10. Plume coordinates.

Measurements were made by tracing the measuring rod and its markings on a transparency then overlaying it onto the individual plume cross section photographs. Figure 11 shows this overlay. Since only half of the outer edge of the plume cross section can be seen during the collapse phase the plume was assumed to be geometrically similar about the X-Y plane.

Dynamic similitude was used to describe the discharge conditions. Principally there were three conditions of concern, two of which had dimensionless relationships. First was a relationship between the mud density and the density of the ambient into which the mud was discharged. This effects the behavior of the dynamic collapse phase of the plume. The densimetric Froude number (Fr), which is the ratio of the mud's inertial force to the ambient's bouyant force, was used to express this relationship.

Second was the relationship of the velocity of the ambient to the mud discharge rate. This was expressed in terms of a velocity ratio, R. The value of this ratio, in part, determines how the mud plume disperses and how fast the plume will fall through the water column. The nominal values for these dimensionless parameters were Fr = 0.40 and R = 0.90.

The salinity gradient, which was discussed earlier in this chapter, is the final condition to consider.

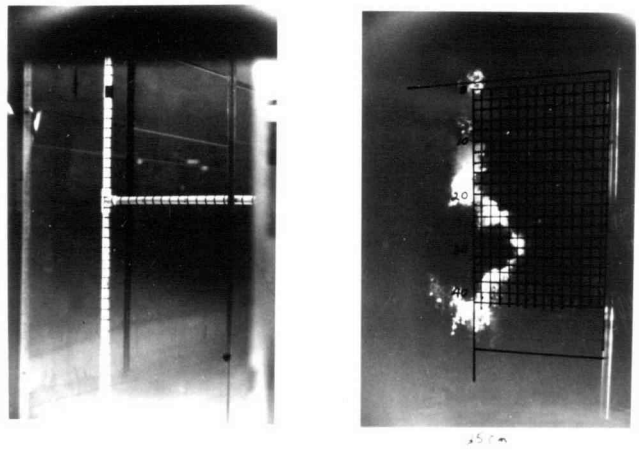

Figure 11. Grid overlay for plume measurement.

RESULTS

This experiment was one of laboratory simulation and measurements. It involved the measurement of a progression of cross sections of the mud plume as it passed from the jet phase into the dynamic collapse phase. The cross sections are physically described by; their relative position to the mud source (discharge tube), their geometric shape, and the discharge conditions. The discharge conditions are found in the appendix. They are described in terms of two dimensionless independent variables, the Froude number and the velocity ratio, and salinity vs. Y/D.

In this chapter the results of runs 6 through 9 are presented graphically. The results shown in figures 12 through 18 are geometrical descriptions of the plume cross sections as they progress through the jet phase to the dynamic collapse phase. The results show that in each of the runs, the collapse begins just after the plume passes below the transition band. In the stronger gradients of runs 6 and 7 the lower edge of the plume immediately begins to rise once the dynamic collapse phase begins. In the weaker gradients of runs 8 and 9 the lower edge of the plume continues to fall a small amount more before rising to its neutral bouyancy. The stronger gradient also causes an earlier and much more definite collapse than the weaker gradient.

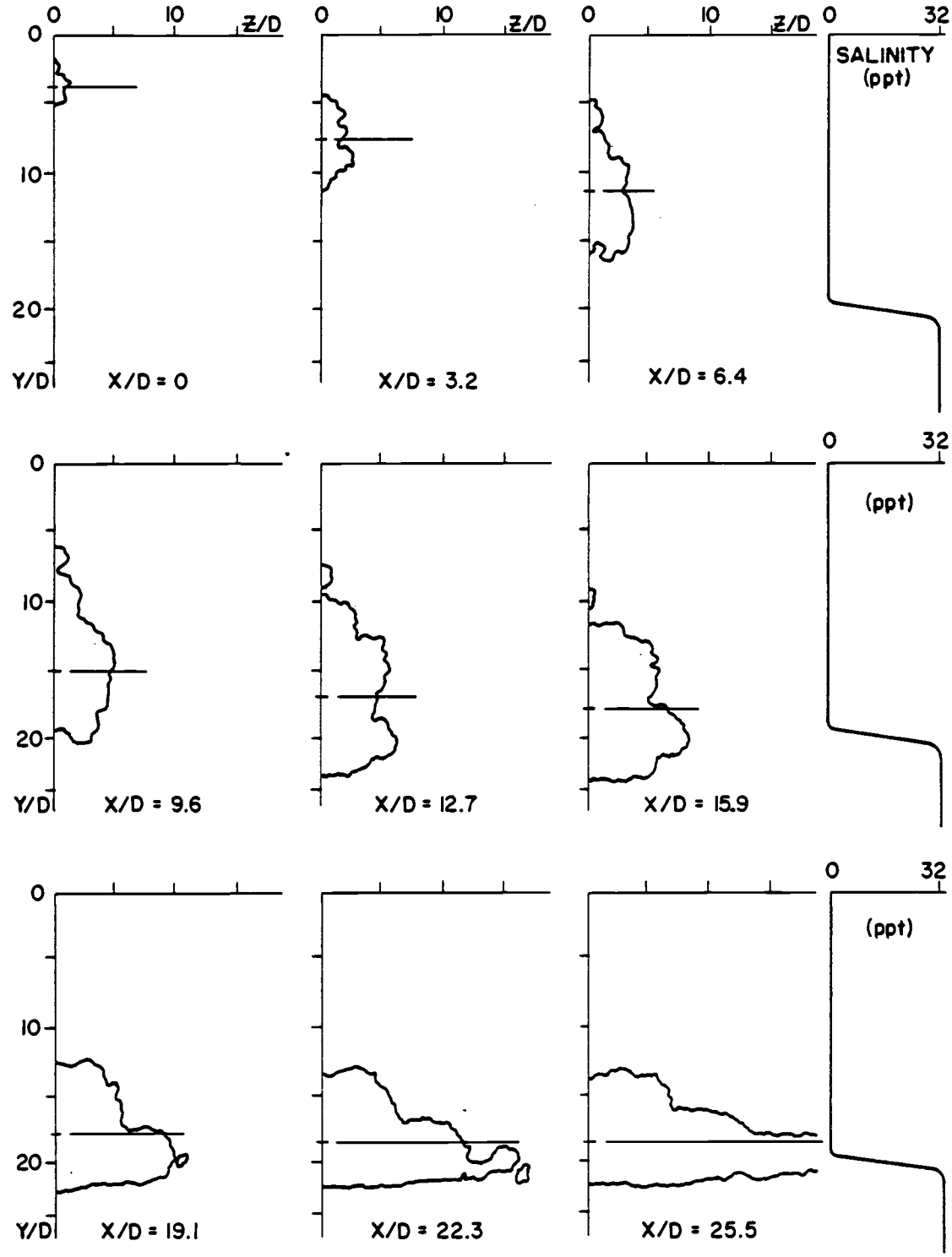

Figure 12. Results for run # 6,
X/D=0.0 to X/D=25.5

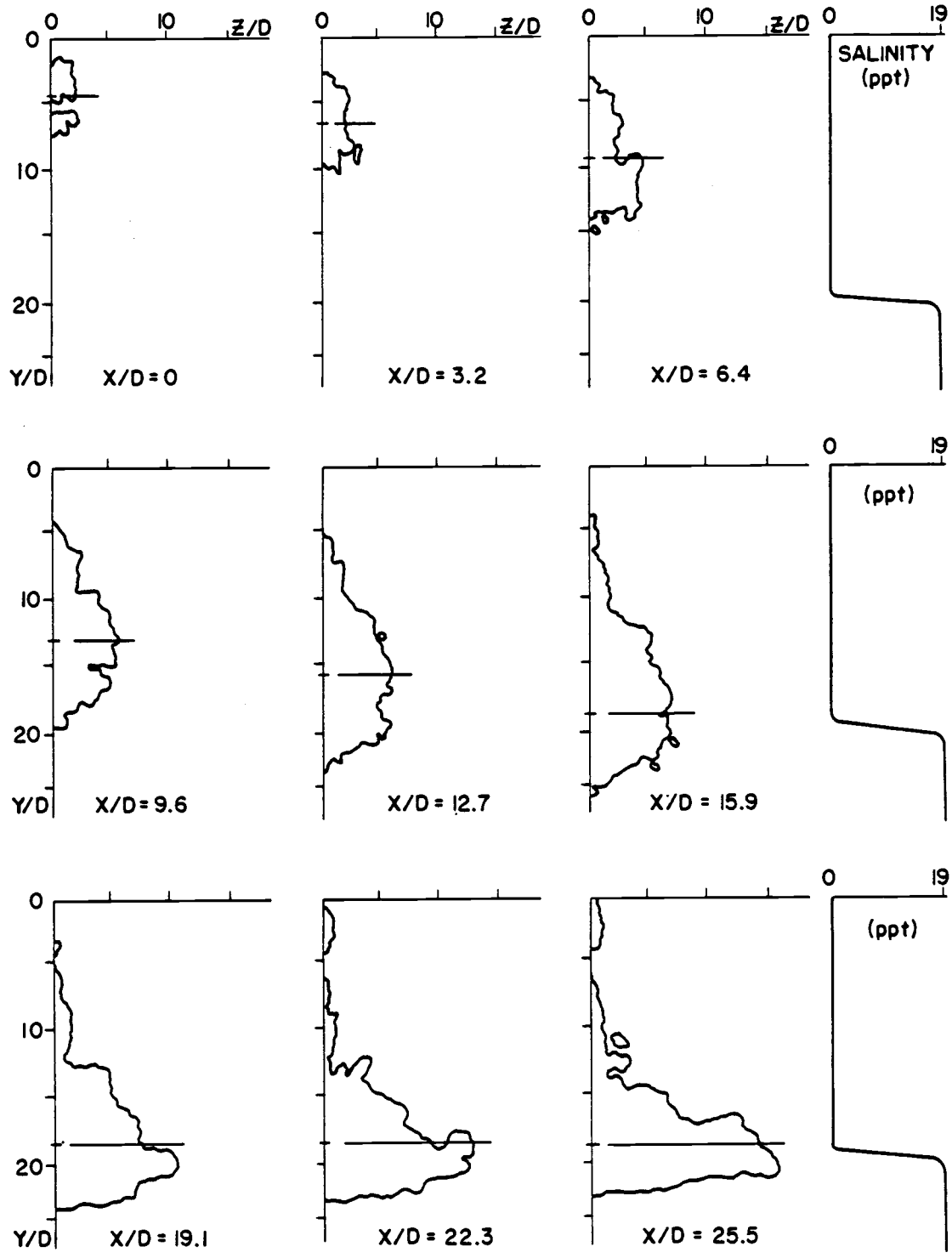

Figure 13. Results for run # 7,
X/D=0.0 to X/D=25.5

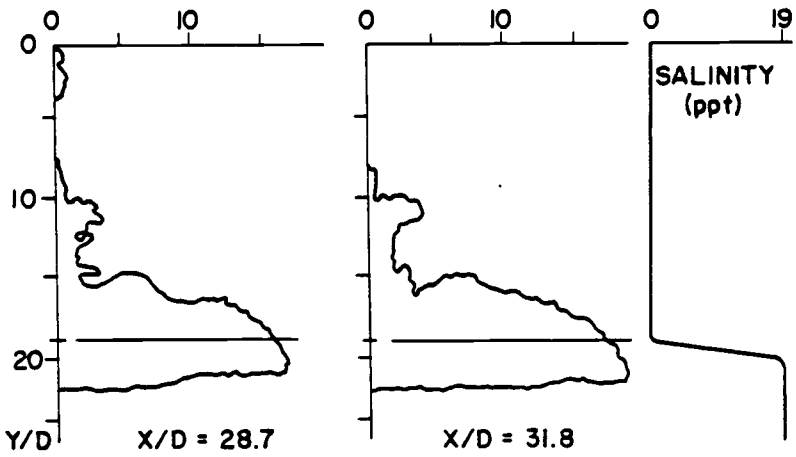

Figure 14. Results for run # 7
X/D=28.7 and X/D=31.8

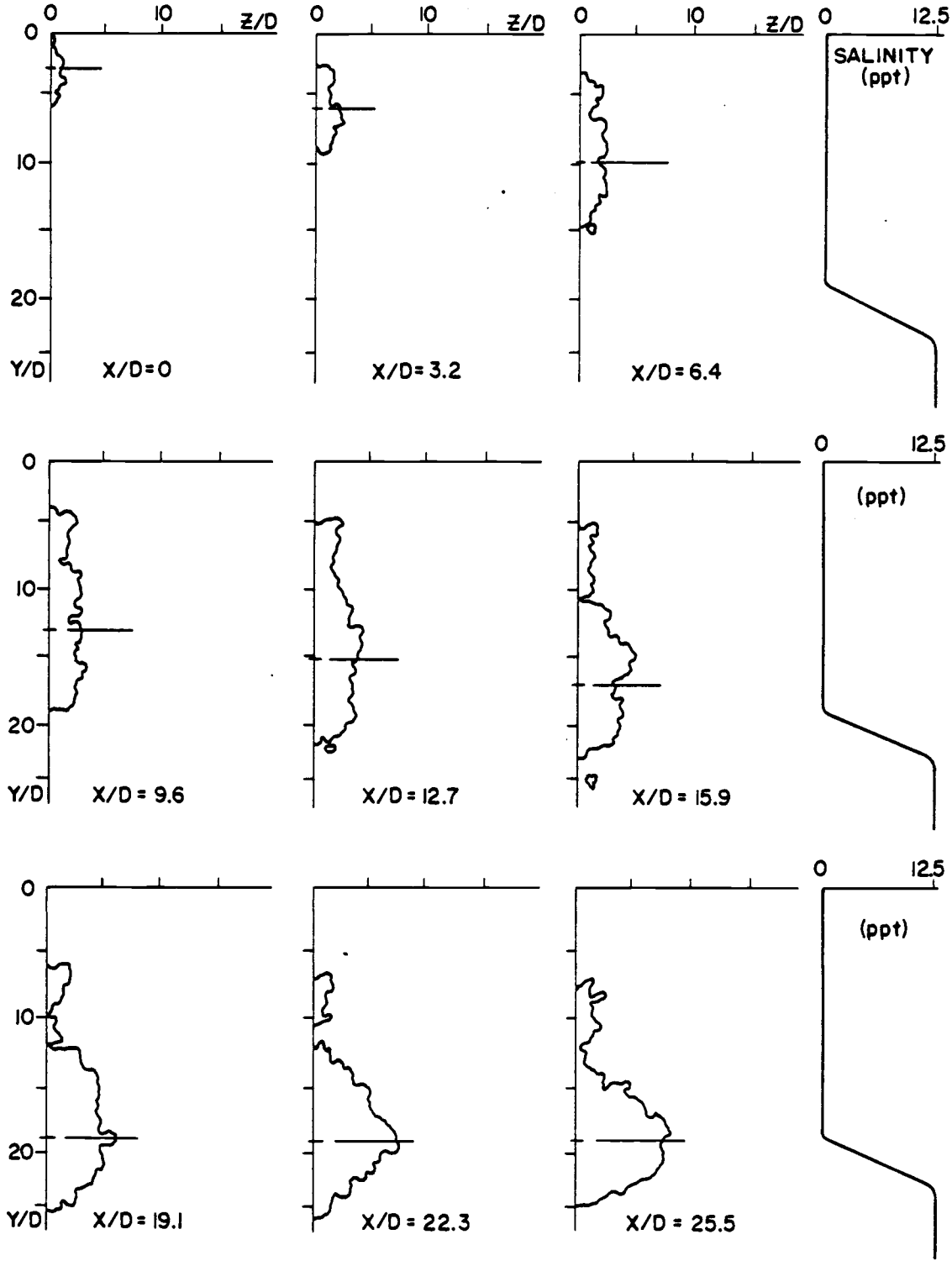

Figure 15. Results for run # 8
X/D=0.0 to X/D=25.5

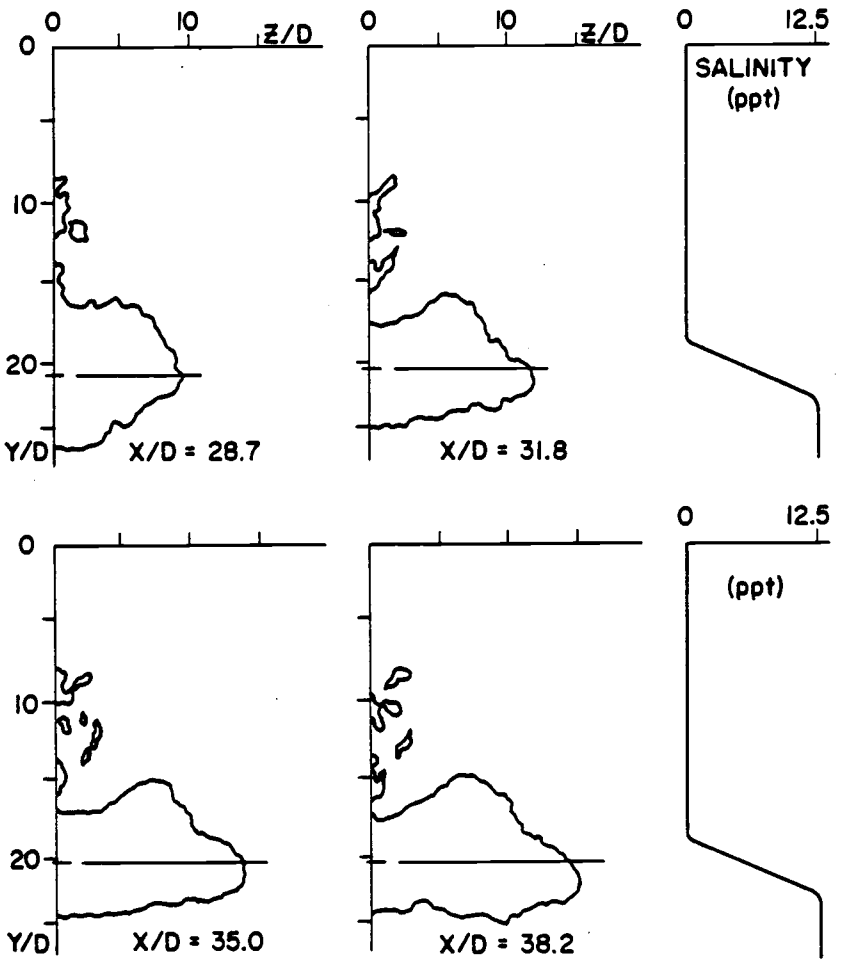

Figure 16. Results for run # 8
X/D=28.7 to X/D=31.8

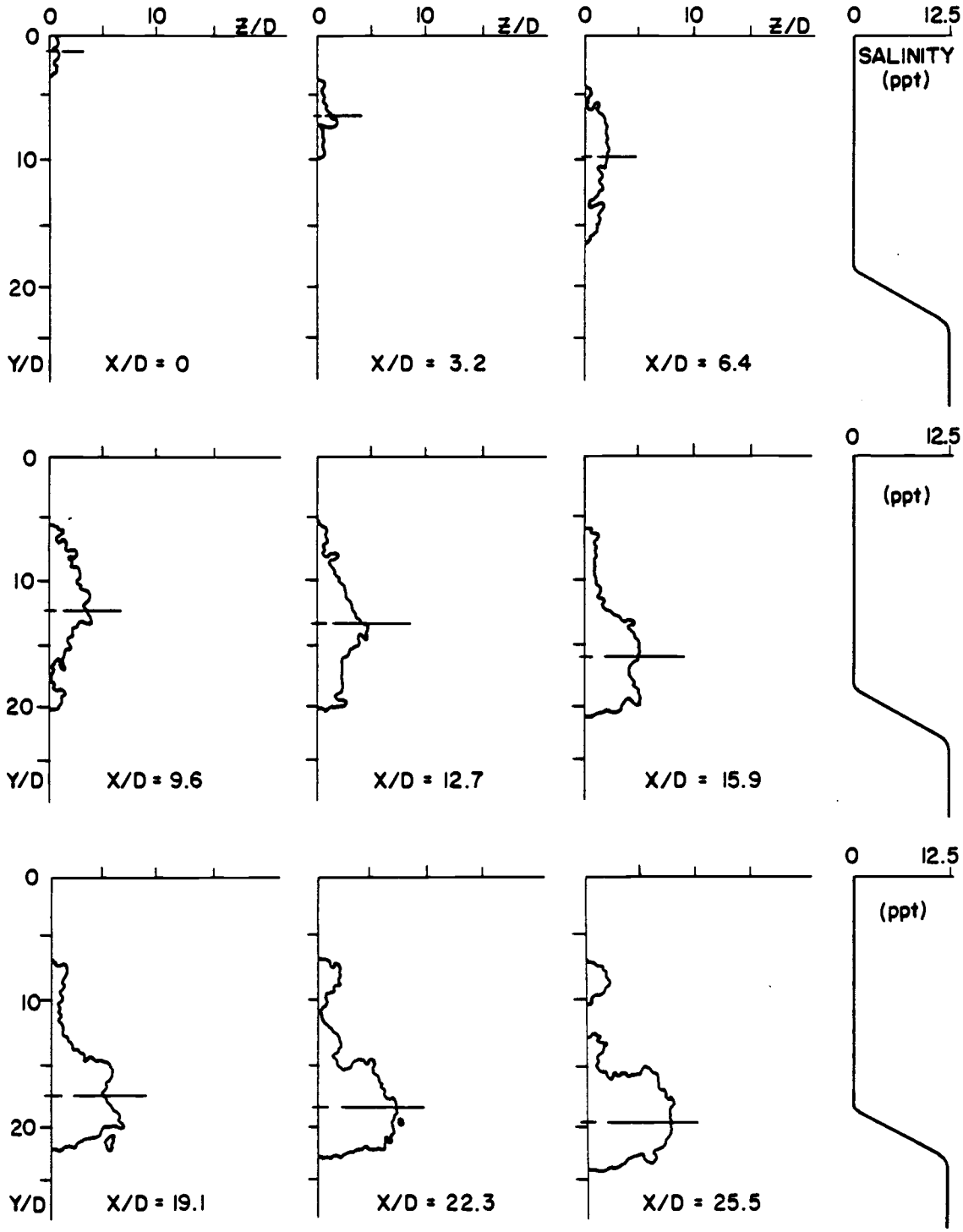

Figure 17. Results for run # 9,
X/D=0.0 to X/D=25.5

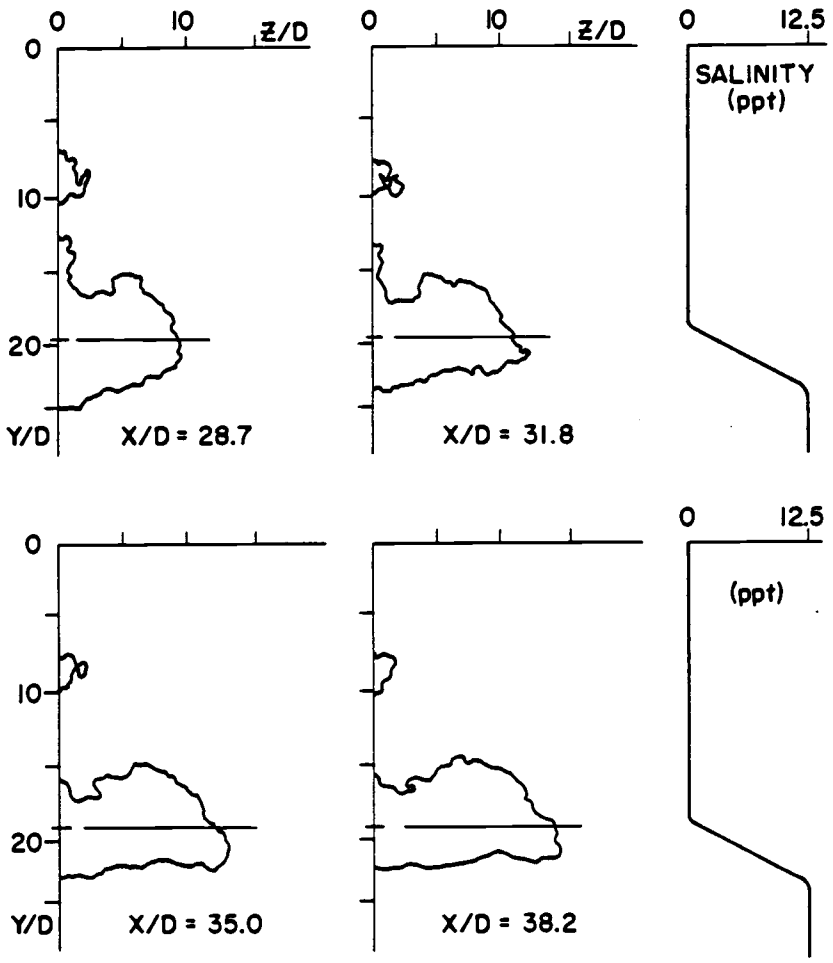

Figure 18. Results for run # 9,
X/D=28.7 to X/D=38.2

Photographs of the plume cross sections were taken from X/D=0.0 to X/D=38.2. In the strongest gradient, run #6, the plume hit the side walls of the tank at X/D=25.5, before the last photograph. The spreading plumes in the weaker gradients of runs #8 and #9 did not reach the side walls until after X/D=38.2. The gradient's effect on plume collapse is further shown in examining differences in the plume's spreading edge at a single location, X/D, for each run. At X/D=22.3, the outer plume edge was at b/D=16.2 for run 6, at b/D=12.7 for run 7 and b/D=7.6 for runs 8 and 9. These differences were partly due to more material settling out of the plume in the weaker gradient and in part due to the greater bouyant forces of the stronger gradient. Figure 19 shows the distance of the outer plume edge, b/D, with respect to the location of the plume cross section, X/D.

Runs 8 and 9 had similar density gradients and thus produced similar results. The collapse phase in both runs started at about X/D=25. From that point, the spreading rates for both plumes are close. Run 8 has a slightly higher spreading rate due to its larger discharge rate. The similarities in runs 8 and 9 show a good consistency in the experimental procedure. The general behavior of all four runs is in good agreement with the behavior of the assumed mud plume as modeled by the OOC computer program.

Error in measurement is inherent in all experimental work. This experiment was no exception. Errors in measuring towing and discharge rates are compounded when describing the discharge conditions in terms of froude number and velocity ratio. The error

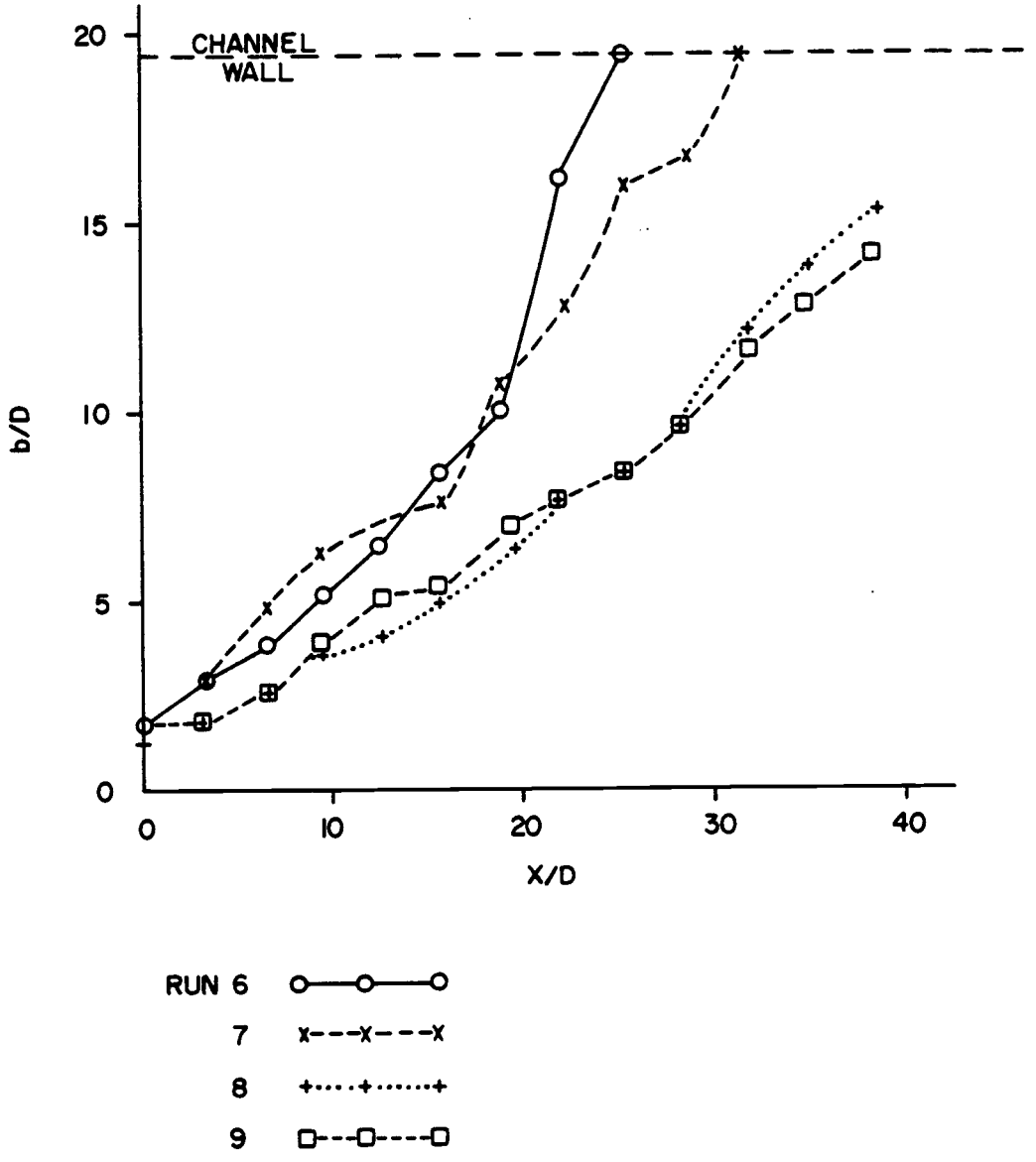

Figure 19. Plot of outer plume edge vs. plume cross-section location for runs 6 through 9.

in these values was determined to be plus or minus ten percent of their values. The values can be found in the appendix.

The error in salinity measurement was caused by a distorted signal on the oscilliscope after the conductivity probe entered the transition region. The acceptability of these errors will have to be determined once comparable results are available from a computer simulation.

CONCLUSIONS

The laboratory simulation of the discharge of drilling mud into a flowing, stratified environment, in general, behaved as anticipated. Upon discharge, the vertically-descending mud plume began to entrain the surrounding fluid as it bent in the direction of flow. The plume reached a level of neutral bouyancy and stopped its descent, at which point a dynamic collapse was observed. During this plume development, heavier solids in the mud plume settled out. Flocculation was observed as the settling material entered the higher density salt water. The OOC discharge model assumes a mud plume phenomenon very similar to the behavior described above.

Other characteristics of the discharged mud were noted in cases of different density gradients. The stronger gradients encouraged a quicker, more deliberate plume collapse than the weaker gradients. This was observed both visually and quantitatively. At distance of X/D=22.3 from the discharge tube, the outer plume edge was at b/D=16.2 in the strongest density gradient and at b/D=7.6 in the weakest density gradient. The photographic technique used proved to be an excellent method for determining plume cross sections at desired X/D locations.

Finally, the procedure of the mud discharge simulation produced reasonably consistent results. Three different density gradients were used in the experimental runs and all three runs exhibited the first two characteristic phases of a fluid discharged

into a flowing stratified environment. These two being the jet phase and the dynamic collapse phase. Runs 8 and 9 showed further consistency in the procedure. Both these runs had similar density gradients and both had plumes which collapsed and spread close to the same time and rate.

This experimental investigation provided good information for comparison with computer simulations. It is suggested that future experiments include a timed automatic shutter release on the camera to reduce the inaccuracy of manual release. Also adjustments should be made to the mud pumping arrangement so a more consistent mud flow could be produced from one run to another giving a more constant Froude number and velocity ratio.

BIBLIOGRAPHY

1. Ray, J.P. and Meek, R.P., Water Column Characterization of Drilling Fluids Dispersion from an Offshore Exploratory Well on Tanner Bank, Research on Environmental Fate and Effects of Drilling Fluids and Cuttings, Symposium Proceedings: Vol. 1, Lake Buena Vista, Florida, January 21-24, 1980

2. Ayers, R.C., Sauer, T.C., Stuebner, D.O. and Meek, R.P., An Environmental Study to Assess the Effect of Drilling Fluids on Water Quality Parameters During High Rate, High Volume Discharges to the Ocean, Research on Environmental Fate and Effects of Drilling Fluids and Cuttings, Symposium Proceedings: Vol. 1, Lake Buena Vista, Florida, January 21-24, 1980

3. Koh, R.C.Y., The Physics and Processes Related to Discharge of Marine Effluents, An Evaluation of Effluent Dispersion and Fate Models for OCS Platforms, Workshop Proceedings: Vol. 1, July, 1983

4. Brandsma,M.G., Davis, L.R., Ayers, R.C. and Sauer, T.C., A Computer Model to Predict the Short Term Fate of Drilling Discharges in the Marine Environment, Research on Environmental Fate and Effects of Drilling Fluids and Cuttings, Symposium Proceedings: Vol. 1, Lake Buena Vista, Florida, January 21-24, 1980

5. Brandsma, M.G., Ayers, R.C. and Sauer, T.C., Mud Discharge Model, Report and User's Guide, Version 1, Exxon Production Research Company, July 1983

6. Davis, L.R., Mohebbi,B, An experimental Investigation of Drilling Fluid Disposal in a Flowing, Stratified Environment, Final Report on Technical Service Agreement for Exxon Production Research Company, PR 6953, June 1983

7. Koh, R.C.Y. and Chang, Y.C., Mathmatical Model for Barged Ocean Disposal of Water, Environmental Protection Technology Series EPA 660/2-73-029, December 1973, U.S. EPA, Washington, D.C.

8. Davis, L.R., Gregoric, M. and Bushnell, D.J., An Experimental Investigation of merging Buoyant Jets in a Crossflow, Journal of Heat Transfer, Vol. 104, No. 2, pp. 236-240, May 1982

APPENDIX

Table 1. Discharge conditions and measurements for run 6.

Discharge Conditions

Fr = 0.41, ±0.03
R = 0.84, ±0.07
Towing rate = 5.29 cm/s
Discharge rate = 6.32 cm/s

Salinity in towing channel

Y/D, 0.4	Salinity, ppt, 0.5
0.0	0.0
19.1	0.0
19.4	3.0
19.7	13.0
20.-	18.0
20.4	28.0
21.7	31.0
22.0	32.0 maximum

Plume Cross Section Geometry

X/D	Y/D	Ymax/D	b/D	$A/(\pi D^2/4)$
0.0	3.8	5.1	1.3	4.1
3.2	7.6	11.5	2.9	26.9
6.4	11.5	16.6	3.8	65.1
9.6	15.3	21.0	5.1	107.4
12.7	16.9	24.2	6.4	165.3
15.9	17.8	24.5	8.3	190.1
19.1	17.8	22.9	10.2	191.1
22.3	18.2	22.6	16.2	232.4
25.5	18.2	22.6	plume hit the wall	
28.7		22.6		
31.8		22.6		
35.0		22.6		
38.2		22.6		

Table 2. Discharge conditions and measurements for run 7.

Discharge Conditions

Fr = 0.49, ±0.03
R = 0.79, ±0.07
Towing rate = 5.97 cm/s
Discharge rate = 7.60 cm/s

Salinity in towing channel

Y/D,	0.4	salinity, ppt,	0.5
0.0		0.0	
19.1		0.0	
19.7		5.0	
20.1		6.5	
20.4		16.5	
20.7		18.5	
21.7		19.0	maximum

Plume Cross Section Geometry

X/D	Y/D	Ymax/D	b/D	$A/(\pi D^2/4)$
0.0	4.1	7.3	1.3	23.2
3.2	6.4	10.2	2.9	36.2
6.4	8.9	14.0	4.8	72.3
9.6	13.1	18.5	6.1	128.1
12.7	15.6	22.9	6.4	165.3
15.9	18.5	24.2	7.0	198.4
19.1	18.8	24.2	10.8	219.0
22.3	18.8	23.9	12.7	239.7
25.5	18.8	23.2	15.9	260.3
28.7	18.8	22.6	16.6	268.6
31.8		22.6	Plume hit the wall	
35.0		22.6		
38.2		22.6		

Table 3. Discharge conditions and measurements for run 8.

Discharge Conditions

Fr = 0.40, ±0.03
R = 0.99 ±0.07
Towing rate = 6.15 cm/s
Discharge rate = 6.23 cm/s

Salinity in towing channel

Y/D	0.4	salinity, ppt,	0.5
0.0		0.0	
18.5		0.0	
19.4		1.0	
19.7		3.0	
20.1		7.0	
20.4		9.5	
20.7		11.0	
21.3		12.0	
22.9		12.0	
24.2		12.5	maximum

Plume Cross Section Geometry

X/D	Y/D	Ymax/D	b/D	$A/(\pi D^2/4)$
0.0	2.9	5.7	1.3	10.3
3.2	5.7	8.9	2.5	23.2
6.4	9.9	14.6	2.5	49.6
9.6	12.7	18.5	3.5	82.6
12.7	14.6	21.7	4.1	115.7
15.9	16.6	22.9	5.1	124.0
19.1	18.5	25.2	6.4	157.0
22.3	19.1	25.8	7.6	170.5
25.5	19.1	26.1	8.3	186.0
28.7	20.7	26.1	9.6	190.1
31.8	20.4	24.8	12.1	198.4
35.0	20.1	24.2	14.0	239.7
38.2	20.1	24.2	15.3	256.2

Table 4. Discharge conditions and measurements for run 9.

Discharge conditions

Fr = 0.36, ±0.03
R = 1.06, ±0.07
Towing rate = 5.90 cm/s
Discharge velocity = 5.57 cm/s

Salinity in towing channel

Y/D, 0.4	salinity, ppt, 0.5
0.0	0.0
17.8	0.0
18.5	1.5
19.1	4.5
19.7	8.5
20.4	10.5
21.0	11.5
21.7	12.0
22.3	12.0
24.2	12.5 maximum

Plume cross section geometry

X/D	Y/D	Ymax/D	b/D	$A/(\pi D^2/4)$
0.0	1.0	2.9	1.0	4.1
3.2	6.4	9.6	1.9	10.3
6.4	9.6	16.6	2.5	37.2
9.6	12.1	20.1	3.8	64.1
12.7	13.4	21.0	5.1	82.6
15.9	15.9	21.7	5.4	103.3
19.1	17.2	22.3	7.0	124.0
22.3	18.2	23.6	7.6	148.8
25.5	19.4	24.2	8.3	169.4
28.7	19.4	24.2	9.6	194.2
31.8	19.1	23.6	11.5	196.3
35.0	18.8	22.9	12.7	210.8
38.2	18.8	22.3	14.0	222.1